COMSOL
CONFERENCE
2023 MUNICH

Numerical Simulation of the One-Way Mechanical-Electrochemical Coupling in Structural Supercapacitors

D. Peyrow Hedayati[1], G. Kahlmeyer[1], M. Kucher[1], R. Böhm[1]
1. Faculty of Engineering, Leipzig University of Applied Sciences, Leipzig, Germany.

Abstract
Multifunctional Energy Storage Composites (MESC) combine the superior structural properties of carbon fiber reinforced polymers (CFRP) with an integrated battery function. As a result, they can have broad aerospace and automotive applications in the future. Structural Supercapacitors (SSC) are an important type of MESC. As integrated structural parts, an SSC is required to retain its electrochemical performance while undergoing mechanical loads. In addition to fiber electrodes, a key ingredient of SSCs is the structural electrolyte. A promising type of structural electrolytes are the bicontinuous porous Solid Polymer Electrolytes (SPE), which comprise a non-conducting stiff epoxy resin skeleton that provides the required mechanical strength; and an ionic liquid (IL) component responsible for the SSC electrochemical function. In SSCs, capacitance depends on the diffusion of the ionic species, which move exclusively through the diffusion paths, i.e. polymer porosities. In other words, the effective diffusion coefficient of a bicontinuous electrolyte relies on the morphological factors of the electrolyte microstructure. Applying mechanical loads can change the electrolyte morphology and hence impact the diffusion process. The current study aims to model and numerically simulate the mechanical-electrochemical coupling in a bicontinuous electrolyte and investigate its effect on the total SSC performance under compressive loads.

Keywords: Structural Supercapacitor (SSC), Solid Polymer Electrolyte (SPE), mechanical-electrochemical coupling, Representative Volume Element (RVE), Cyclic Voltammetry (CV)

1. Introduction
Multifunctional energy storage composites (MESC) are integrated structural batteries (SB) or structural supercapacitors (SSC) which replace conventional carbon fiber reinforced polymer composite (CFRP) to carry load and store electrical energy simultaneously. SSCs have wide potential applications and can result in large reductions in structural mass [1, 2]. In an SSC, carbon fibers have the dual responsibilities of carrying mechanical load (reinforcement function) and maintaining electron conduction (electrode function). Another crucial component of SSC is the structural electrolyte which is required to have both high stiffness and high ionic conductivity [3]. Gel polymer electrolytes are typically used as structural electrolyte, but have poor load carrying capacity [3]. On the other hand, porous Solid Polymer Electrolytes (SPE) with a bicontinuous microstructure present the advantage of high load transfer (matrix function) while providing ion conductivity (electrolyte function). This is achieved through an intermingled liquid-solid system with superior multifunctional performance, in which the polymer skeleton is flooded with ionic liquid electrolyte[4], as shown in Figure 1. A mechanically robust bicontinuous electrolyte has been recently developed by Shirshova et al. [3]. It contains 30 wt.% structural resin and 70 wt.% ionic liquid electrolyte, and has a room temperature ionic conductivity of 0.8 $mS.cm^{-1}$ and a Young's modulus of 0.2 GPa.

The mechanical-electrochemical interactions in such structural electrolytes can have synergistic or parasitic effects on the global SSC performance and therefore needs to be studied. At the moment, there is little knowledge about the mechanical-electrochemical coupling in these systems. Several studies have experimentally reported on the effect of mechanical stress on structural batteries and supercapacitors [5, 6]. Furthermore, a coupled electrochemical-mechanical model is formulated for solid polymer electrolytes by Grazioli et al. [7] to investigate the impact of mechanical stresses on the Li-ion battery performance. However, a modeling framework to explain the coupling effect involved in bicontinuous porous SPE is not reported to the best of the authors' knowledge.

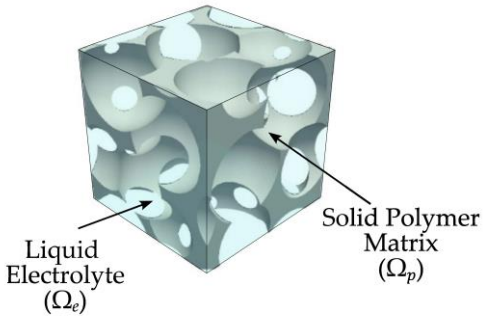

Figure 1. Schematic illustration of the numerically generated inverse bead model (from [4]) of a bi-continuous SPE consisting of a polymer solid phase (Ω_p) flooded with an ionic liquid phase(Ω_e).

In this work, the effect of mechanical loading on a bicontinuous structural electrolyte is investigated using a coupled model.

Methodology

The proposed coupled mechano-electrochemical model and the associated workflow applied in this work is shown in Figure 2. At first, a simplified statistically-representative 2D micromodel of the porous polymer structure was generated. Various compressive strains ($\varepsilon = 0, 2, 4, 6, 8, 10\%$) were then applied using COMSOL Multiphysics structural mechanics interface. The emerging deformation plots were further analyzed to measure morphological properties of interest (i.e. porosity (φ) and tortuosity (τ)) using image processing techniques. The two parameters were used to calculate the effective diffusion coefficient at every strain value. Finally, this data was then fed back to COMSOL Multiphysics electroanalysis interface to simulate the cyclic voltammetry (CV) of the SSC.

CV is a useful analytical tool to investigate the electrochemical systems. Using this approach, the potential difference between a working electrode and a reference electrode is swept linearly in time from a minimum to a maximum potential in cycles. The resulting current at the working electrode is recorded and is plotted against the applied electrode potential in a voltammogram.

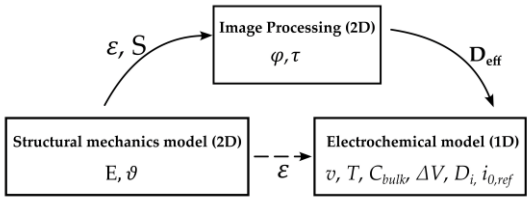

Figure 2. Mechanical-electrochemical modeling framework used in this study.

Mechanical-Electrochemical Coupling

In the following sections, the mechanical-electrochemical modeling of the system along with governing equations and conditions in two domains are presented. According to Figure 1, the two distinct domains are the polymer matrix domain (Ω_p), and the ionic liquid domain (Ω_e).

Structural Mechanics Modeling

In this study, a linear elastic constitutive model is employed for the mechanical description of an isotropic polymer matrix using the numerically-efficient homogenization technique.

Computational Homogenization

The global response of a porous SPE is controlled by the complex phenomena which occur at lower scales. Therefore, multi-scale theories that transfer information between macro and microscales have to be adopted to predict the macroscopic constitutive response of the SSC [7]. An effective tool for a realistic prediction of material behavior is the computational homogenization method using representative volume element (RVE) [8]. In this study, a 2D square-shape RVE ($L_i \times L_i$) and constant boundary conditions are chosen based on scanning electron microscopy (SEM) images of the electrolyte (Figure 3a). The RVE is assumed to statistically represent the SPE microscale configuration. Hill-Mandel principle of macrohomogeneity [9] is assumed to be applicable here since the microstructural length (µm) scale is sufficiently smaller than the SPE characteristic macroscale length (mm) [10]. The RVE of the bicontinuous SPE was simplified to a numerically-generated inverse bead model, according to [4] (Figure 3b). Furthermore, the microstructural geometry is also assumed to have local periodicity [8].

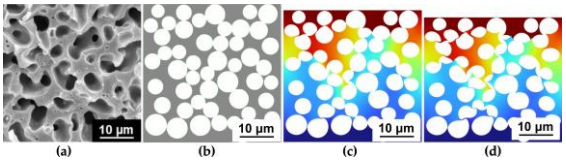

Figure 3. (a) Scanning electron microscopy of the bicontinuous SPE [3], (b) the corresponding inverse bead RVE, and deformation plots at (c) ε=5%, and (d) ε=10%

Governing equations

Linear elastic constitutive relations model the reversible behavior of a material that is subjected to infinitesimal strains. This model is valid for deformations up to approximately 10% [7]. Equation of motion according to the Newton's second law in stationary mode (i.e. equilibrium equation) is as follows:

$$\nabla \cdot \boldsymbol{S} + \boldsymbol{F}_V = 0 \qquad \text{in } \Omega_p \times \mathbb{R}^+ \qquad (1)$$

Next, is the strain-displacement equation:

$$\boldsymbol{\varepsilon} = \frac{1}{2}[\nabla \mathbf{u} + (\nabla \mathbf{u})^T] \qquad \text{in } \Omega_p \times \mathbb{R}^+ \qquad (2)$$

And finally, the Hooke's law:

$$\mathbf{S} = \mathbf{C} : \boldsymbol{\varepsilon} \qquad \text{in } \Omega_p \times \mathbb{R}^+ \qquad (3)$$

In the above set of equations, $\boldsymbol{S}$ is the Cauchy stress tensor, $\boldsymbol{\varepsilon}$ is the infinitesimal strain tensor, $\mathbf{u}$ is the displacement vector, $\mathbf{C}$ is the fourth-order stiffness tensor, and $\boldsymbol{F}_V$ is the body force per unit volume.

Boundary and initial conditions

The linear elastic traction boundary condition requires:

$$\mathbf{n} \cdot \boldsymbol{S} = \boldsymbol{t}^* \qquad \text{in } \Omega_p \times \mathbb{R}^+ \qquad (4)$$

where $\mathbf{n}$ is the outer unit normal vector on the elastic body and $\boldsymbol{t}^*$ is the stress vector. The displacement boundary condition is:

$$\mathbf{u} = \boldsymbol{u}^* \qquad \text{in } \Omega_p \times \mathbb{R}^+ \qquad (5)$$

in which $\boldsymbol{u}^*$ is the prescribed displacement field.

The solid mechanics module in COMSOL Multiphysics 6.0 was used for the numerical solution

of the linear elastic deformation in the bicontinuous SPE at various strain steps.

Electrochemistry Modeling

Certain assumptions to simplify the underlying equations in cyclic voltammetry was used in the current study. The model is reduced to one-dimensional (1D) electro-diffusion for all ion species. The material properties obtained from RVE-size architecture are applied in the model to account for the morphological changes in the SPE. The binary electrolyte solution is KCl. It is assumed that the initial diffusion coefficient of both species is constant and equal. The length domain is the maximum extent of the diffusion layer over the duration of the voltammetry experiment [11] and is given by:

$$\lambda = \sqrt{6 D_{\text{eff}} t_{\max}} \qquad \text{in } \Omega_e \times \mathbb{R}^+ \quad (6)$$

Here, D_{eff} is the effective diffusion coefficient of the reactant and $t_{\max}$ is the duration of the cyclic voltammogram.

A common approximation to solve voltammetry physical equations is to consider a large electrode (macroelectrode) which has uniform transport behavior across its surface [12]. As a result, only the physics occurring normal to the surface need to be considered. Furthermore, in this model, a parametric sweep is used to compare voltammetry recorded at a fixed voltammetry scan rate but different effective diffusion coefficients.

Governing equations

An important assumption in this section is the unstirred nature of the electrolyte solution (at least after the deformation is complete) which means convection is nonexistent. It was also assumed that a large quantity of supporting electrolyte is present. Under these conditions, the resistance of the solution is sufficiently low that the electric field is negligible, and we can assume $\phi_l = 0$.

The Electroanalysis interface in COMSOL Multiphysics implements chemical transport equations for the reactant and product species of the redox couple subject to this assumption.

The governing equation is the diffusion equation (also known as Fick's second law) to describe the chemical transport of the electroactive species A and B. It is assumed that a large amount of electrolyte is present at the electrode-electrolyte interface.

Based on the assumptions made above, the voltammetry analysis translates into a time-dependent problem with uniform reactions and transport phenomena across the electrode surface. As a result, the diffusion of the species within the thin layer (λ) is described by the Fick's second law [11]:

$$\frac{\partial c_i}{\partial t} = D_i \frac{\partial c_i}{\partial x} \qquad \text{in } \Omega_e \times \mathbb{R}^+ \quad (7)$$

in which c_i is the species concentration.

Boundary and initial conditions

Due to the electroneutrality assumption:

$$c_i(\lambda, t) = c_{\text{bulk}} \qquad \text{in } \Omega_e \times \mathbb{R}^+ \quad (8)$$

At the electrode boundary ($x = 0$), the following electrochemical reaction between reactant species (A) and product (B) takes place:

$$B + e^- \leftrightarrow A$$

The current density j_{loc} for this reaction is given by the electroanalytical Butler-Volmer equation for an oxidation[12]:

$$j_{\text{loc}} = nFk_0\left(c_A \exp\left(\frac{(n-\alpha_c)F\eta}{RT}\right) - c_B \exp\left(\frac{-\alpha_c F\eta}{RT}\right)\right) \qquad \text{in } \Omega_e \times \mathbb{R}^+ \quad (9)$$

where k_0 is the heterogeneous rate constant of the reaction, $\eta = \Delta E - E_{eq}$ is the overpotential. α_c is the transfer coefficient for the cathodic process. In equation above, n is the number of transferred electrons (here, $n = 1$).

The reactant and product species flux across the electrode surface ($\boldsymbol{N}$) is given by the Faraday's law of electrolysis (Electrode Surface boundary condition) :

$$-\boldsymbol{n}.\boldsymbol{N}_i = \frac{v_i i_{loc}}{nF} \qquad \text{in } \Omega_e \times \mathbb{R}^+ \quad (10)$$

where $\boldsymbol{n}$ is the surface normal and v is the scan rate, which is the rate at which the applied potential is changed.

The applied triangular waveform for the cyclic voltammetry study is specified in the electrode surface boundary condition according to two vertex potentials forming a potential window between –0.4 V and +0.4 V and is given by [13]:

$$E(t) = \begin{cases} E_{\min} + vt, & t < t_0 \\ E_{\max} - v[t - t_0], & v \le t < 2t_0 \end{cases} \qquad \text{in } \Omega_e \times \mathbb{R}^+ \quad (11)$$

where $t_0 = 2(E_{max} - E_{min})/v$ is the cycle period.

Finally, in 1D, the total current is related to the current density multiplied by the electrode area A:

$$I_{\text{el}} = i_{loc} A \qquad \text{in } \Omega_e \times \mathbb{R}^+ \quad (12)$$

The electroanalysis interface in COMSOL Multiphysics 6.0 was used to simulate cyclic voltammetry of the bicontinuous electrolyte. The parameters used are summarized in the appendix (Tables A1 and A2).

Effective Diffusion

Ionic diffusion in the bicontinuous SPE, as a porous heterogeneous material, is not identical with diffusion in a fully solid or liquid electrolyte. Therefore, effective values need to be used. To describe the effective diffusion coefficient, we employ a popular phenomenological model as described below [14].

$$D_{\text{eff}} = \kappa D_{bulk} \qquad \text{in } \Omega_e \times \mathbb{R}^+ \quad (13)$$

where the diffusion factor κ is given by:

$$\kappa = \frac{\varphi}{\tau} \qquad \text{in } \Omega_p \times \mathbb{R}^+ \quad (14)$$

In the above equation, φ and τ are porosity and tortuosity of the porous RVE, respectively and are given by the below equations:

$$\varphi = \frac{A_{\text{pore}}}{A_{\text{total}}} \qquad \text{in } \Omega_p \times \mathbb{R}^+ \qquad (15)$$

$$\tau = \frac{L_g}{L} \qquad \text{in } \Omega_p \times \mathbb{R}^+ \qquad (16)$$

In equation 15, A_{pore} and A_{total} refer to the pore and total areas of the RVE, respectively. L_g and L are the shortest pore channel and straight line distances in the RVE, respectively, as shown in equation 16. While porosity measures the ratio of the void spaces in materials, tortuosity is a ratio that characterizes the convoluted pathways of fluid diffusion and ionic conduction through porous media [15]. In the context of mechanical-electrochemical coupling or an SSC under mechanical loading, these two important factors cannot be assumed as fixed constants and should be treated as deformation-dependent variables. This fact is the cornerstone of the coupling methodology in this work. Figure 4 shows the evolution of tortuosity and porosity in the RVE before and after 10% strain. In this figure, the black and white colors represent the solid resin and the pores (or ionic liquid space), respectively. The red line shows the shortest possible ionic conduction path. Subscripts *i* and *f* refer to the initial and final deformed states.

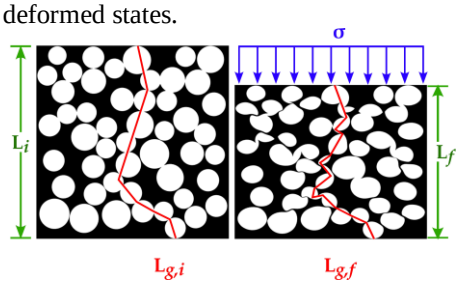

Figure 4. Morphological evolution of the porous SPE before (left) and after 10% compressive strain (right).

Results and Discussion

The shape of the simulated cyclic voltammogram (Figure 5) shows the relation between electrode kinetics and diffusion-controlled chemical species transport.

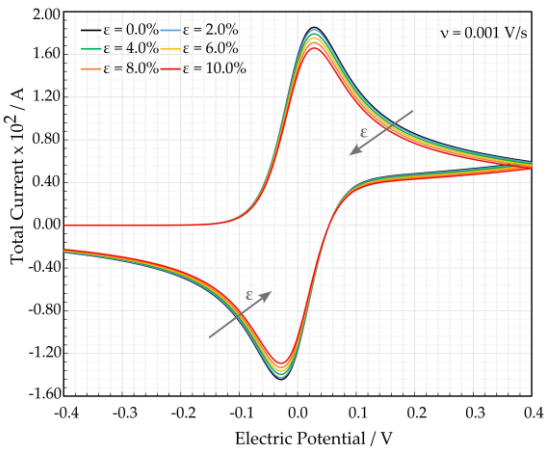

Figure 5. Cyclic voltammetry recorded at a macroelectrode for various compressive strains.

Initially, at reducing potentials, the oxidation reaction does not happen and the drawn current is small. At higher potentials, the oxidation reaction is accelerated and the current increases. Once the oxidation reaction has consumed the reactant at the electrode surface, the current becomes limited by the rate of transport of A toward the working electrode. Therefore, a peak current is seen, and at higher potentials, the voltammetric current drops at a potential-independent rate. On sweeping back toward more reducing potentials, the reconversion of the product B into the original reactant A gives a negative current. Depletion of the reacting species B leads to a negative peak current after which the reconversion proceeds at a diffusion-controlled rate. The as-deformed microstructure after each strain was then captured from COMSOL Multiphysics and transferred to the ImageJ software [15] to measure the tortuosity. Porosity measurements were carried out in a Python code developed by the authors. Deformations plots of the RVE at selected strain levels of ε = 5%, and ε = 10% are shown in Figure 2c-d. The pre and post deformation morphological parameters are summarized in Table 1. An important observation was that upon application of strains greater than 10%, the conduction path at the RVE became non-existent ($\tau = \infty$). This phenomenon can be referred to as a "*battery micro failure mode*", in which the battery function of the MESC fails while the structure is still at infinitesimal strains.

***Table 1**: Morphological parameters of the porous SPE before and after deformation.*

Strain (%)	Porosity (%)	Tortuosity	κ factor
0.0	52.14	1.21	0.43
2.0	51.55	1.22	0.42
4.0	50.25	1.27	0.40
6.0	48.38	1.28	0.38
8.0	47.40	1.31	0.36
10.0	46.37	1.35	0.34

The effective diffusion coefficient at various strains was calculated using equations 8-10 and the data in Table 1. The corresponding simulated cyclic voltammetry for each strain is projected in Figure 5. As figure 5 suggests, increasing the compressive strain shrinks the inner area of the CV curve. In addition, cyclic voltammogram can be used to calculate the specific capacitance using the below equation:

$$C_s = \frac{1}{2mv\Delta V}\int_{V_0}^{V} I(V)dV \qquad (17)$$

where m is the mass of active material on the electrode in gram, v is the scan rate, ΔV is the potential window and $\int_{V_0}^{V} I(V)dV$ is the area under the CV curve [16]. The values of specific capacitance at each strain is presented in Table 2.

***Table 2**: Morphological parameters of the porous electrolyte before and after deformation.*

Strain (%)	Area under CV (AV)	Specific capacitance (kF/g)
0.0	59.92	2.71
2.0	59.21	2.68
4.0	57.92	2.62
6.0	56.64	2.56
8.0	55.25	2.50
10.0	53.62	2.42

Energy density ($\bar{\Gamma}$) is an important parameter which shows the available electrical energy content per kilogram of SSC. Using the specific capacitance calculated above, energy density $\bar{\Gamma}$ can also be calculated using the following relation:

$$\bar{\Gamma} = \frac{1}{2} C_s (\Delta V)^2 \qquad (18)$$

Figure 6, shows the changes in energy density of an SSC with bicontinuous SPE against increasing strain.

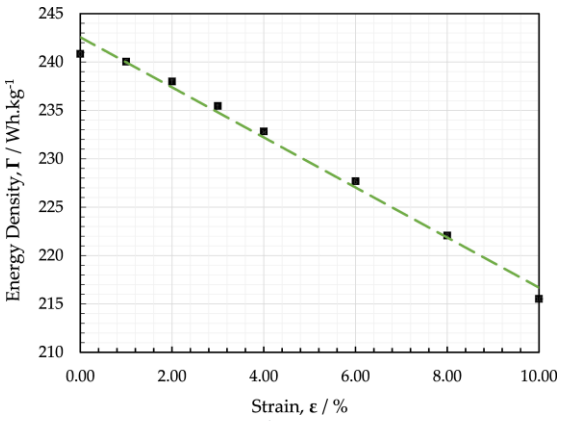

Figure 6. Energy density of the SSC with bicontinuous SPE versus the applied compressive strain.

According to Figure 6, increased compressive strain in the porous SPE resulted in noticeable decrease in the SSC's energy density. This can be explained by the fact that the compressive stress deforms the polymer skeleton which results in a change in its morphology. As an outcome, the available ion conductive pathways evolve leading to a change in the effective diffusion coefficient of the electrolyte. In this particular case, deformations led to a decreased diffusion coefficient, which resulted in lower specific capacitance values (see Figure 5). This translates into a lower energy density for the SCC. On the contrary, experimental studies on SSCs with fully aqueous electrolyte reported an increase in specific capacitance when exposed to compression loads [6, 17]. This can be explained by the electrolyte nature in porous SPE and conventional liquid electrolytes. While increasing compressive load shortens the ionic diffusion path between electrodes in a liquid electrolyte, a porous solid electrolyte has a more complex structure that behaves differently upon applied stress. This emphasizes the critical role of electrolyte morphology in the SCC design for load-bearing applications.

Conclusions and Future Work

In this study, a coupled mechanical-electrochemical model was proposed to investigate the effect of mechanical loads on the energy density of a structural supercapacitor with a bicontinuous polymer electrolyte. The model is based on the dependence of effective ionic diffusion on the morphological features of the structural electrolyte. Separate mechanical and electrochemical simulations were carried out on a representative volume element using COMOSL Multiphysics software and image processing tools. The results showed that in a porous polymer electrolyte, increasing the compressive strains up to 10% lowers the energy density of the SSC by around 12%. Future efforts will focus on validating the model with experimental data.

References

[1] D. Peyrow Hedayati, M. Kucher, H. Biggs, and R. Böhm, "Application of structural energy storage devices in aerial monitoring systems: a conceptual design study," in Belfast, B. G. Falzon and C. McCarthy, Eds., 2023.

[2] D. Peyrow Hedayati, G. Singh, M. Kucher, T. D. Keene, and R. Böhm, "Physicochemical Modeling of Electrochemical Impedance in Solid-State Supercapacitors," *Materials (Basel, Switzerland)*, early access. doi: 10.3390/ma16031232.

[3] N. Shirshova *et al.*, "Structural supercapacitor electrolytes based on bicontinuous ionic liquid–epoxy resin systems," *J. Mater. Chem. A*, vol. 1, no. 48, p. 15300, 2013. doi: 10.1039/C3TA13163G.

[4] V. Tu, L. E. Asp, N. Shirshova, F. Larsson, K. Runesson, and R. Jänicke, "Performance of bicontinuous structural electrolytes," *Multifunct. Mater.*, vol. 3, no. 2, p. 25001, 2020. doi: 10.1088/2399-7532/ab8d9b.

[5] Andrew S. Westover, John Tian, Shiva Bernath, Landon Oakes, Rob Edwards, Farhan Nur Shabab, Shahana Chatterjee, Amrutur Anilkumar, Cary L. Pint, "Multifunctional Load-Bearing Energy Storage Materials,"

[6] X. Li, J. Rong, and B. Wei, "Electrochemical behavior of single-walled carbon nanotube supercapacitors under compressive stress," *ACS nano*, vol. 4, no. 10, pp. 6039–6049, 2010, doi: 10.1021/nn101595y.

[7] D. Grazioli, O. Verners, V. Zadin, D. Brandell, and A. Simone, "Electrochemical-mechanical modeling of solid polymer electrolytes: Impact of mechanical stresses on

Li-ion battery performance," *Electrochemical Acta*, vol. 296, pp. 1122–1141, 2019, doi: 10.1016/j.electacta.2018.07.234.

[8] K. Terada, M. Hori, T. Kyoya, and N. Kikuchi, "Simulation of the multi-scale convergence in computational homogenization approaches," *International Journal of Solids and Structures*, vol. 37, no. 16, pp. 2285–2311, 2000. doi: 10.1016/S0020-7683(98)00341-2.

[9] J. Bishop and R. Hill, "XLVI. A theory of the plastic distortion of a polycrystalline aggregate under combined stresses," *The London, Edinburgh, and Dublin Philosophical Magazine and Journal of Science*, vol. 42, no. 327, pp. 414–427, 1951, doi: 10.1080/14786445108561065.

[10] W. F. dos Santos, I. A. Rodrigues Lopes, F. M. Andrade Pires, and S. P. Proença, "Second-order multi-scale modelling of natural and architected materials in the presence of voids: Formulation and numerical implementation," *Computer Methods in Applied Mechanics and Engineering*, vol. 416, p. 116374, 2023, doi: 10.1016/j.cma.2023.116374.

[11] A. Lavacchi, U. Bardi, C. Borri, S. Caporali, A. Fossati, and I. Perissi, "Cyclic voltammetry simulation at microelectrode arrays with COMSOL Multiphysics®," *J Appl Electrochem*, vol. 39, no. 11, pp. 2159–2163, 2009. doi: 10.1007/s10800-009-9797-2.

[12] A. J. Bard and L. R. Faulkner, *Electrochemical methods: Fundamentals and applications*, 2nd ed. New York, Weinheim: Wiley, 2001.

[13] H.-L. Girard, H. Wang, A. d'Entremont, and L. Pilon, "Physical Interpretation of Cyclic Voltammetry for Hybrid Pseudocapacitors," *J. Phys. Chem. C*, vol. 119, no. 21, pp. 11349–11361, 2015, doi: 10.1021/acs.jpcc.5b00641.

[14] L. Shen and Z. Chen, "Critical review of the impact of tortuosity on diffusion," *Chemical Engineering Science*, vol. 62, no. 14, pp. 3748–3755, 2007. doi: 10.1016/j.ces.2007.03.041.

[15] M. B. Clennell, "Tortuosity: a guide through the maze," *SP*, vol. 122, no. 1, pp. 299–344, 1997, doi: 10.1144/GSL.SP.1997.122.01.18.

[16] S. Sharma and P. Chand, "Supercapacitor and electrochemical techniques: A brief review," *Results in Chemistry*, vol. 5, p. 100885, 2023. doi: 10.1016/j.rechem.2023.100885.

[17] W. Sun, Y. Zhang, and F. Yang, "A High-Performance Symmetric Supercapacitor from Porous Activated Carbon under Compression," *Energy Tech*, vol. 9, no. 5, p. 2100068, 2021, doi: 10.1002/ente.202100068.

Acknowledgements

The research was funded by the M-Era.net project "Next Generation of 3D Printed Structural Supercapacitors" (PRINTCAP), Contract Number 100633785. This project is co-financed by public taxes from the budget approved by the Saxon State Parliament.

Appendix

Parameters used in both electroanalysis and structural mechanics simulation are given in tables A1 and A2, respectively.

***Table A1**: List of parameters for the electroanalysis simulation*

Parameter	Value	Unit	Description
v	1×10^{-3}	V/s	Voltammetric scan rate
c_{bulk}	1.05×10^{3}	mmol/L	Reactant bulk concentration
D_A	1×10^{-9}	m^2/s	Reactant diffusion coefficient
D_B	1×10^{-9}	m^2/s	Product diffusion coefficient
K_0	1×10^{10}	-	Reaction rate
r_e	10	mm	Electrode radius
$i_{0,\text{ref}}$	9.6485×10^{10}	A/m^2	Reference exchange current density
C_{dl}	0.2	F/m^2	Double layer capacitance
T	298.15	K	Temperature
E_{min}	-0.4	V	Start potential
E_{max}	0.4	V	Switching potential

***Table A2**: List of parameters for the structural simulation*

Parameter	Value	Unit	Description
L_i	60	µm	Initial quadratic RVE length
E	3.86	GPa	Young's Modulus of the pure Epoxy
ν	0.45	-	Poisson ratio
ρ	1.19×10^{3}	kg/m^3	Epoxy Density